Journal of Materials Chemistry C

PAPER

View Article Online
View Journal | View Issue

Cite this: J. Mater. Chem. C, 2014, 2, 2251

High refractive index transparent nanocomposites prepared by *in situ* polymerization†

Chieh-Ming Tsai,[a] Sheng-Hao Hsu,‡[b] Chun-Chih Ho,[a] Yu-Chieh Tu,[a] Hsin-Chien Tsai,[b] Chung-An Wang[a] and Wei-Fang Su*[ab]

Received 8th December 2013
Accepted 7th January 2014

DOI: 10.1039/c3tc32374a

www.rsc.org/MaterialsC

High refractive index transparent nanocomposites have been developed by *in situ* polymerization of a precursor that contains functional monomers and surface modified anatase TiO_2 nanoparticles for optoelectronic applications. The monomers are in the liquid form, so environmentally friendly solventless precursors can be prepared. The precursor can be processed into various shapes or thick films (>50 microns) of the nanocomposite. The relationships of the chemical structure of the organic matrix, nanoparticle content and dispersity with the refractive index, transparency, mechanical and thermal properties are systematically investigated. The refractive index, and mechanical and thermal properties of the nanocomposite are increased with increasing TiO_2 content and aromatic structure in the organic matrix due to their rigid characteristics. The transparency of the nanocomposite is increased with increasing TiO_2 content and dispersity. At the same loading of nanoparticles, the higher dispersity and the better transparency are due to the less extent of Rayleigh scattering. At 18 vol% (60 wt%) of TiO_2, the acetic acid modified TiO_2/poly(4-vinyl benzyl alcohol) nanocomposite has a refractive index of 1.73 and excellent transparency (>85% from 500 nm to 800 nm). The refractive index of the nanocomposite can be further increased to 1.77 by replacing aliphatic acetic acid modified TiO_2 with aromatic phenyl acetic acid modified TiO_2. The results of this work provide new knowledge and a new pathway to design a polymer based high refractive index material.

Introduction

High refractive index materials have wide applications in optics, such as optical lenses, polarizers, filters and waveguides. The material can also be applied to photovoltaics and semiconductor manufacturing.[1] The high refractive index encapsulation layer and antireflection layer for light emitting diodes or solar cells can improve the efficiency of devices.[2,3] A thin transparent film of a few microns has reached a refractive index higher than 1.9 from a solvent based polymer–nanoparticle system by the solution process.[4–8] However, the process has pollution problem from the solvent and it is difficult to obtain a thick film of more than 50 microns. Very few reports exist on solventless systems that can form a transparent bulk or thick film with a refractive index higher than 1.7.[9–13]

TiO_2–polymer hybrid systems have been extensively studied as high refractive index materials. Polyacrylate, polyimide, polysilane, and epoxy polymers were used in the systems.[4,7,9,14–21] The nanoparticles of anatase TiO_2 are often used because rutile TiO_2 with a higher refractive index is difficult to synthesize with a size smaller than 50 nm.[19] The small size of nanoparticles is required for the synthesis of highly transparent nanocomposites due to minimized scattering effects. The hydrophilic TiO_2 is very difficult to be dispersed in the hydrophobic polymer. The dispersity and chemical inertness of TiO_2 can be modified by inorganic coatings such as ZrO_2.[11] The ZrO_2 separates the organic matrix and TiO_2 to avoid aggregation. The organic coating on TiO_2 has been proved to be a more effective way to eliminate aggregation. The coating can be easily obtained from organic ligand modified TiO_2. In general, two approaches are utilized to obtain ligand-modified TiO_2. One is to synthesize the nanoparticles in ligands such as oleic acid or triethanolamine, so the ligand modified nanoparticles are formed in a one step process. The other is a two-step process.[7,22] The surface of nanoparticles is modified after the formation of nanoparticles. The modifier can be acids, amines, alcohols, silanes, phosphonates, sulfonates and so on.[6,12,13,15,19,23–25] A combination of more than two different approaches is also feasible such as TiO_2–ZrO_2–acrylic acid.[12]

[a]Department of Materials Science and Engineering, National Taiwan University, Taipei, Taiwan, 106. E-mail: suwf@ntu.edu.tw; Fax: +886-2-23634562; Tel: +886-2-33664078

[b]Institute of Polymer Science and Engineering, National Taiwan University, Taipei, Taiwan

† Electronic supplementary information (ESI) available. See DOI: 10.1039/c3tc32374a

‡ Current address: Graduate Institute of Clinic Dentistry, School of Dentistry, National Taiwan University, Taipei, Taiwan.

In this research, we used a one-step approach to make nanoparticles of aromatic phenyl acetic acid modified TiO_2 (PAA–TiO_2) and aliphatic hexanoic acid modified TiO_2 (HA–TiO_2) that are compatible with poly(ethoxylated (6) bisphenol A dimethacrylate). We employed a two-step approach to make acetic acid modified TiO_2 (AA–TiO_2) compatible with poly-(4-vinyl benzyl alcohol). According to the Lorentz–Lorenz equation, when the material has larger density or smaller molar volume, the refractive index is higher.[26]

To predict the refractive index of the nanocomposite, its effective refractive index can be calculated by the summation of the volume fraction of each component multiplied with its refractive index according to the mixing rule as shown below.

$$n = \sum_{i}^{N} n_i \quad (1)$$

where n_i is the equivalent refractive index of the i component at its volume fraction. The polymer containing planar aromatic structure is easier to be packed densely as compared with the polymer containing only a flexible zigzag aliphatic structure. Thus, we postulated that the nanocomposite containing a high amount of aromatic structure in the organic matrix and high content of inorganic nanoparticles will exhibit a high refractive index. The effects of the content of nanoparticles on the refractive index, transparency, mechanical and thermal properties of the nanocomposite were systematically investigated. The effect of the chemical structure of the ligand and the polymer on the refractive index value was also carefully studied. The precursor of the nanocomposite is in the liquid form without any solvent that can be *in situ* polymerized into nanocomposites *via* UV radiation or heat. A thick cast film with a refractive index of 1.77 has been achieved for the first time to our knowledge without using toxic solvents and heavy metal based nanoparticles such as PbS.[17]

Experimental

Chemicals

Phenyl acetic acid (PAA, 98.5%), hexanoic acid (HA, 99%), titanium isopropoxide (TTIP, 98%), tetrabutyl ammonium bromide (Bu_4NBr, 99%), and 4-vinyl benzyl chloride (4-VBzCl, 90%) were obtained from ACROS (Geel, Belgium). Acetic acid (AA, 99.7%) and magnesium sulphate (99.7%) were obtained from Fisher (Hampton, USA). Ethoxylated (6) bisphenol A dimethacrylate ($EO_{(6)}$BDMA, SR-541) was obtained from Sartomer (Exton, USA). 2,2-Dimethoxy-1,2-di(phenyl) ethanone (Irg 651, 99%) was obtained from Ciba (Basel, Switzerland). Azobis(isobutyronitrile) (AIBN, 99.8%) was obtained from Aldrich (St. Louis, USA).

Synthesis of PAA or HA surface-modified TiO_2

Either 90 mL hexanoic acid (HA) or 98 g phenyl acetic acid (PAA) was added into a three-neck flask, and heated to 120 °C under stirring for 30 min to remove water. After decreasing the temperature to 78 °C, 8 mL titanium isopropoxide (TTIP) was added to the flask. 10 min later, 14.4 mL deionized water was added to the flask and reacted at 98 °C for 24 hours. The solution was washed with methanol, and then centrifuged at 4000 rpm for 2 min three times. The particles were dispersed in chloroform to make about a 1 wt% light yellow clear solution. The two nanoparticles were named as HA–TiO_2 and PAA–TiO_2 according to the ligands of HA and PAA respectively.

Synthesis of AA surface-modified TiO_2

48.6 g TTIP and 12 g acetic acid (AA) were well mixed for 15 min, and then the mixture was injected into a three-neck flask containing 290 mL water in nitrogen under stirring. After 1 hour, 4 mL nitric acid was added into the solution. The solution was heated to 78 °C in 40 min, which took another 75 min to react. After cooling, the aqueous solution of nanoparticles was obtained and stored at room temperature, we named it AA–TiO_2.

Synthesis of 4-vinyl benzyl alcohol (VBzOH)[26]

95 g tetrabutyl ammonium bromide (Bu_4NBr) and 1.2 g NaOH in 750 mL H_2O were added into 50 g 4-vinyl benzyl chloride. The mixture was heated at 125 °C for 1 hour and subsequently cooled in an ice/water bath. After cooling, the mixture was extracted with 750 mL ethyl acetate (EA) three times and the combined organic layers were dried with $MgSO_4$, filtered, concentrated and purified by column chromatography (CombiFlash Torrent) (EA : hexane = 1 : 5) to give a product of light yellow oil. We named it VBzOH in short. The molecular weight of VBzOH is 119. The VBzOH contains one mole of aromatic structure per mole of VBzOH.

Preparation of solventless TiO_2/acrylate nanocomposite precursors

The acid surface-modified TiO_2 solution, ethoxylated (6) bisphenol A dimethacrylate ($EO_{(6)}$BDMA) and photo-initiator (Irgacure 651) were mixed together and stirred for 30 min first. And then the solvent was removed under vacuum at 10^{-3} Torr for two hours. The resultant nanocomposite precursors with HA or PAA modified TiO_2 nanoparticles were named as E–HT series or E–PT series respectively. The first letter of denotation indicates the type of surface modifier, the second letter indicates the TiO_2 nanoparticle, and the third letter represents the type of monomer, for instance E means $EO_{(6)}$BDMA. We added the number after the denotation which indicated the weight percentage of nanoparticles. Their compositions are listed in Table 1.

Preparation of solventless TiO_2/VBzOH nanocomposite precursors

The AA–TiO_2 aqueous solution was rotary evaporated to remove most of the nitric acid, and then specific amounts of 4-vinyl benzyl alcohol (VBzOH) and ethanol were added into the concentrated TiO_2 solution. After rotary evaporation, adding ethanol and sonication for several times, azobis(isobutyronitrile) (AIBN) and methanol were added. The solvent was removed under vacuum (10^{-3} Torr for one hour). The resultant nanocomposite precursors with different TiO_2 ratios were called

Table 1 Compositions of TiO_2/polyacrylate and TiO_2/polyVBzOH nanocomposite precursors

	Composition(wt%)						
Sample name	$EO_{(6)}BDMA$	VBzOH	HA–TiO_2	PAA–TiO_2	AA–TiO_2	Irgacure 651	AIBN
Neat acrylate	96.15	0	0	0	0	3.85	0
E–HT20	76.92	0	20	0	0	3.08	0
E–HT40	57.69	0	40	0	0	2.31	0
E–HT50	48.08	0	50	0	0	1.92	0
E–HT60	38.46	0	60	0	0	1.54	0
E–PT20	76.92	0	0	20	0	3.08	0
E–PT40	57.69	0	0	40	0	2.31	0
E–PT50	48.08	0	0	50	0	1.92	0
E–PT60	38.46	0	0	60	0	1.54	0
Neat VBzOH	0	99.5	0	0	0	0	0.5
VB–AT20	0	79.6	0	0	20	0	0.4
VB–AT40	0	59.7	0	0	40	0	0.3
VB–AT60	0	39.8	0	0	60	0	0.2
VB–HT60	0	39.8	60	0	0	0	0.2
VB–PT60	0	39.8	0	60	0	0	0.2

the VB–AT series. A means the acetic acid surface modifier, T indicates TiO_2, and VB represents 4-vinyl benzyl alcohol. Their compositions are also listed in Table 1.

Either PAA–TiO_2 or HA–TiO_2 nanoparticles were also mixed with VBzOH in this experiment for higher refractive index precursors. VBzOH and AIBN were added into the chloroform solution of either of the nanoparticles, and then the solvent was removed *via* vacuum at 10^{-3} Torr.

Fabrication of TiO_2/polyacrylate and TiO_2/poly(vinyl benzyl alcohol) nanocomposite films

Two strips of 60 μm thick 3M 810D Scotch® tape separated by 2 cm were attached onto the glass or silicon wafer substrates as spacers. The nanocomposite precursor was cast between the spacers and isolated from air by a PET film. Then the TiO_2/acrylate precursors were cured using a high-powered UV-lamp box (935 W m^{-2}, OPAS XLite 400Q) with two-minute exposure at a distance of 20 cm and the TiO_2/VBzOH precursor was cured at 75 °C for 24 h. The thicknesses of resultant samples were measured using a Stylus Profiler (Alpha stepper, Veeco Dektak 6M), and they were about 50 μm.

Characterization of materials

The crystallinity of nanoparticles was measured by X-ray powder diffraction (XRD, PANalytical X′ Pert PRO). The fully dried nanoparticle powders were placed into a quartz holder and then the top surface of the powder was flattened by pressing a covering glass on it. The scattering peak can be detected and collated with a standard. The TEM (JOEL JEM-1230) was used to study the size and shape of nanoparticles and to investigate the morphology of the nanocomposite. Samples of nanoparticles were made by a droplet of dilute nanoparticle solution (<0.01 wt%) on a 200 mesh copper grid with a Formvar/carbon support film. The unnecessary solution was absorbed by tissue and then dried at 50 °C. The ultra thin films of the TEM nanocomposite sample were prepared at room temperature by ultra-microtomy (Leika EM UC6 ultra-microtome machine and Drukker ultra-microtome knife). The cutting edge of 35° was used to obtain about an 80 nm film sample that was then placed on the 200 mesh copper grid.

The chemical structure of 4-vinyl benzyl alcohol was determined by ^{1}H NMR (BRUKER AVANCE 400 MHz). The following peaks were found to be identical to those in the literature: δ = 7.26–7.42 (m, ArH, 4H), 6.69–6.76 (m, CH═CH_2, 1H), 5.74–5.78 (d, CH═CH_2, 1H), 5.24–5.27 (d, CH = CH_2, 1H), 4.66–4.69 (s, CH_2, 2H), 2.03–2.06 (s, OH, 1H).[27]

The refractive index of the nanocomposite was evaluated using a prism coupler using a 633 nm laser (Metricon 2010). The 50 μm thick film was cast on a Si wafer, and then the sample was fixed between a pneumatically-operated coupling head and the prism. By rotating the rotary table, we obtained the angle of incidence when the coupling happened, and then the refractive index of the sample was determined.

The transparency of the nanocomposite was evaluated by UV-visible spectroscopy (Perkin Elmer Lambda 35). The 50 μm thick film cast on the glass slide was used in the test. The glass slide was used as a blank sample. The transmittance between the wavelength of 350 nm and 800 nm was measured.

The glass transition temperature (T_g) of the nanocomposite and the heat of reaction of the nanocomposite precursor were determined using a differential scanning calorimeter (DSC, TA DSC Q200). The decomposition temperature (T_d) of the nanocomposite and the amount of organic on the TiO_2 nanoparticles were determined by thermogravimetric analysis (TGA, TA TGA Q800). The TGA test was performed by heating the samples from room temperature to the temperature at which the weight of the samples remained constant. T_d is expressed as the temperature at which the sample lost 5% weight upon heating.

The mechanical properties were measured using a nano-indentation system (CSIRO UMIS II). A Berkovich diamond indenter was used in this study.

Results and discussion

Materials

The chemical structures of organic ligands and monomers are illustrated in Fig. 1. TiO_2 nanoparticles were synthesized by a sol–gel method, and then they were modified with different organic ligands. The surface modified TiO_2 nanoparticles were blended with monomers to make precursors of nanocomposites. The precursor was polymerized *in situ* to form nanocomposites either by UV radiation or heat. The preparation procedures of nanocomposites are detailed in the Experimental section.

Characterization of TiO_2 nanoparticles

Fig. 2 shows the XRD spectra of different surface modified TiO_2 nanoparticles. Compared with the standard TiO_2 spectrum, PAA–TiO_2, HA–TiO_2 and AA–TiO_2 are all in the anatase phase. Fig. 3(a) and (b) show the shape and size of PAA–TiO_2 and HA–TiO_2 respectively. They are very similar; both have a particle size of about 5–15 nm, and a puncheon-like structure. Fig. 3(c) shows the AA–TiO_2 nanoparticles which are much more like spheres than PAA–TiO_2 and HA–TiO_2 with 3–10 nm sized particles. The amount of surface ligands on the TiO_2 nanoparticles was determined by TGA (ESI Fig. S1†), and the amount was 58.22 vol% for PAA–TiO_2, 51.31 vol% for HA–TiO_2 and 51.97 vol% for AA–TiO_2. There are appreciable amounts of ligands on the TiO_2 nanoparticle which will have a large effect on the properties of nanocomposites (discussed later).

Properties of TiO_2/polyacrylate nanocomposites

Table 2 summarizes the physical and thermal properties of different nanocomposites. The refractive index of the nanocomposite increases with increasing the loading of TiO_2 nanoparticles as expected. The E–PT series and E–HT series are TiO_2/polyacrylate nanocomposites. For the E–PT series

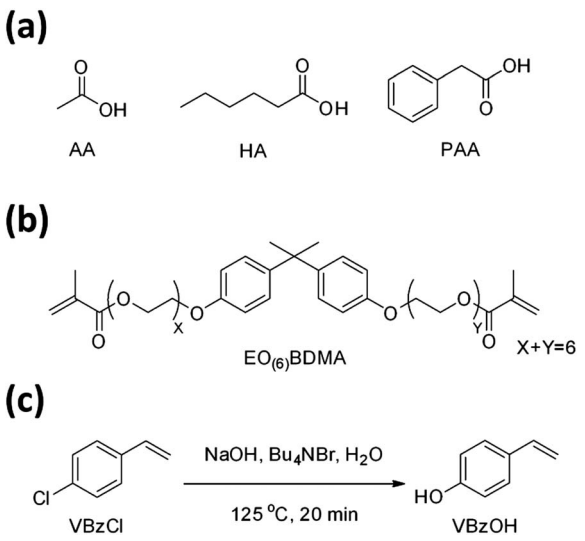

Fig. 1 Chemical structures of (a) surface ligands and (b) $EO_{(6)}BDMA$; (c) the synthetic scheme of VBzOH.

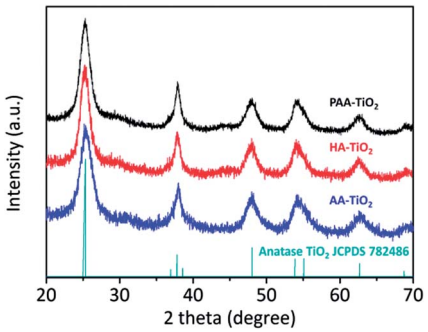

Fig. 2 XRD patterns of different surface-modified TiO_2.

nanocomposites, the relationship between the refractive index and the amount of PAA–TiO_2 is shown in Fig. 4(a). The experimental data (black curve) are in good agreement with the calculated data (red curve) from eqn (1). The results indicate that the PAA–TiO_2 nanoparticles were densely packed in the polyacrylate matrix. The refractive index of the nanocomposite can reach up to 1.70 when it contains 18 vol% of TiO_2. However, Fig. 4(b) shows that the experimental data (black curve) of the nanocomposite of the E–HT series are not in good agreement with the calculated data (red curve) especially at the high loading of HA–TiO_2. The long alkyl chain of HA as compared with the aromatic PAA may be responsible for the results, because the radius of gyration and free volume of HA from its long chain structure are larger. In other words, the HA–TiO_2 could not be densely packed as PAA–TiO_2, with the lax layer whose refractive index is close to that of air (RI = 1), leading to the deviation from the calculated value. The refractive index of the E–HT nanocomposite is lower than that of the E–PT nanocomposite; only 1.67 is reached for the E–HT nanocomposite with a loading of 20.4 vol% HA–TiO_2. The results support our hypothesis that the aromatic ligand will give a higher refractive index nanocomposite than the aliphatic ligand because the aromatic structure could pack densely.

The transparency of nanocomposites was studied by transmission spectroscopy as shown in Fig. 5. For both E–PT series and E–HT series, the nanocomposite exhibits decreased transmission as compared with the neat polymer due to the scattering effect of aggregated nanoparticles and the refractive index difference between nanoparticles and the polymer. The scattering behaviour decreases when the content of nanoparticles increases due to the decrease of the extent of refractive index difference in the material. However, the high amount of nanoparticles in the organic matrix will make the viscosity of the material too high to be processed by casting. There is an optimal amount of nanoparticles that can be present in the organic matrix to have a workable system. The TiO_2 can be increased up to 20.4 vol% for the E–HT60 sample, the transmittance is increased to 65% at a wavelength of 400 nm, then steadily increased to 78% at 800 nm. On the other hand, when the TiO_2 is increased to optimal 18.0 vol% for the E–PT60 sample, the transmittance is increased to 45% at 400 nm and then increased rapidly to 80% at 800 nm. It is interesting to note that the scattering behaviours are quite different between the

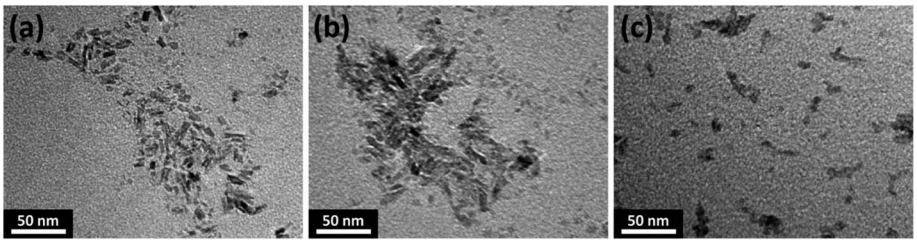

Fig. 3 TEM images of (a) HA–TiO_2 nanoparticles, (b) PAA–TiO_2 nanoparticles, and (c) AA–TiO_2 nanoparticles.

Table 2 Summary of the refractive index, mechanical and thermal properties of nanocomposites

	Properties			
Sample	Refractive index	Hardness (VHN)	T_d (°C)	T_g (°C)
Neat acrylate	1.55	9.45	323.1	53.1
E–HT20	1.58	11.02	299.5	51.6
E–HT40	1.63	12.28	289.2	54.4
E–HT50	1.64	13.41	287.2	56.7
E–HT60	1.67	14.39	277.8	61.8
E–PT20	1.59	13.45	289.6	56.2
E–PT40	1.65	16.30	287.4	58.0
E–PT50	1.68	17.57	286.6	61.7
E–PT60	1.70	19.02	284.7	64.8
Neat VBzOH	1.61	18.76	195.0	43.8
VB–AT20	1.65	25.78	249.6	44.7
VB–AT40	1.69	29.95	233.3	50.2
VB–AT60	1.73	30.61	227.8	52.3
VB–HT60	1.71	12.93	253.0	52.9
VB–PT60	1.77	13.04	270.9	53.4

E–PT series and the E–HT series. At low ~5 vol% TiO_2 (~20 wt %), both nanocomposites show Rayleigh scattering (dependent on the wavelength) from small size aggregates due to the presence of the large refractive index difference in the material (*i.e.* it contained a large amount of polymer). When the loading of TiO_2 is higher than 5 vol%, Rayleigh scattering remains in the E–PT series nanocomposites (Fig. 5(a)). On the other hand, the scattering becomes Mie scattering (independent of the wavelength) for the E–HT series nanocomposites (Fig. 5(b)). The differences result from the difference in the dispersity of TiO_2 nanoparticles in polyacrylate. The dispersity was studied by TEM as shown in Fig. 6. The results indicate that ligand-modified nanoparticles are not fully compatible with the polymer that results in aggregation. The dispersity of PAA–TiO_2 (Fig. 6(a–c)) is worse than that of HA–TiO_2 (Fig. 6(d–f)) in polyacrylate. The size of the aggregates is smaller, and then the extent of aggregation is higher for the E–PT series nanocomposites as compared with the E–HT series nanocomposites. Therefore, the scattering in the E–PT series is dominated by Rayleigh scattering at all PAA–TiO_2 nanoparticle loadings. For the HA–TiO_2 loading above 10 vol% in the E–HT series, the scattering becomes Mie scattering due to the less extent of small size aggregations.

As shown in Table 2, the hardness of both E–PT series and E–HT series nanocomposites increases with the increasing loading of TiO_2 nanoparticles. The result is expected due to the high hardness of inorganic nanoparticles. The degree of increase in hardness of the E–PT series is higher than that of the

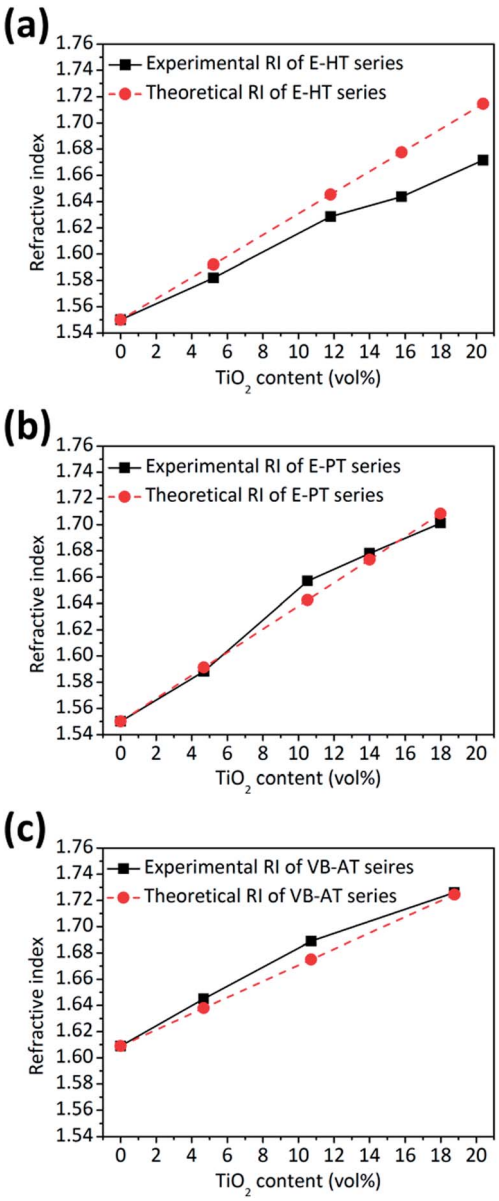

Fig. 4 Experimental and theoretical refractive indices of (a) HA–TiO_2/polyacrylate (E–HT series), (b) PAA–TiO_2/polyacrylate (E–PT series) and (c) AA–TiO_2/poly(4-vinyl benzyl alcohol) (VB–AT series).

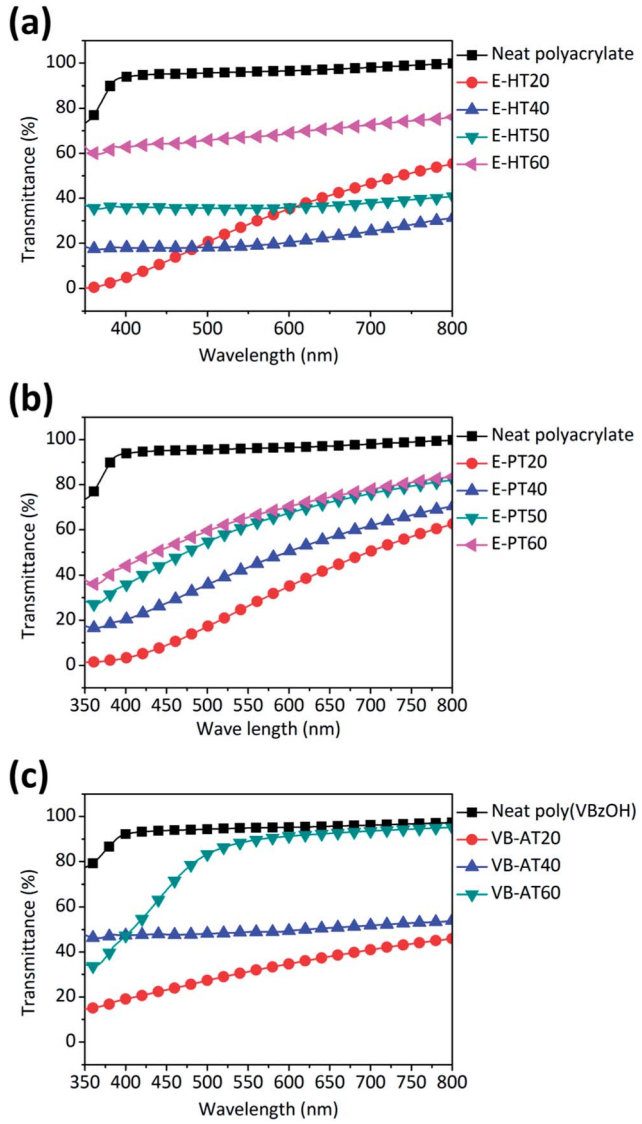

Fig. 5 Transmittance spectra of (a) the HA–TiO_2/polyacrylate nanocomposite (E–HT series) and (b) the PAA–TiO_2/polyacrylate nanocomposite (E–PT series) and (c) AA–TiO_2/poly(4-vinyl benzyl alcohol) (VB–AT series).

E–HT series because the aromatic structure of ligand PAA is more rigid as compared with the flexible alkyl chain of HA. The same reason can explain the higher T_g shown in the E–PT series as compared with the E–HT series (ESI Fig. S2†). The T_g of both series also increases with increasing the loading of TiO_2 because the dense inorganic TiO_2 nanoparticles retard the motion of the nanocomposite upon heating. However, the T_d decreases with increasing the loading of nanoparticles (ESI Fig. S3†). The surface ligand is not chemically bonded with the polymer matrix so the small molecule ligand is decomposed upon heating. At a low TiO_2 loading of ~5 vol%, the PAA ligand decomposes faster than the HA ligand which may be due to the fact that HA–TiO_2 is better dispersed in the polymer, leading to slow decomposition. The degree of decrease in T_d for both series becomes the highest at the loading of TiO_2 close to 20 vol%. The degree of decrease in T_d for E–HT60 is higher than that of E–PT60, because the aliphatic HA is less thermally stable than the aromatic PAA.

Properties of TiO_2/poly(vinyl benzyl alcohol) nanocomposites

In order to increase the refractive index of TiO_2/polyacrylate further, we replace the poly(ethoxylated (6) bisphenol A dimethacrylate) with poly(vinyl benzyl alcohol) to make the TiO_2/poly(vinyl benzyl alcohol) nanocomposite. The aromatic structure of nanocomposites can be increased from 0.3 mol% to 0.8 mol% after the replacement of polyacrylate with poly(vinyl benzyl alcohol). The aqueous AA–TiO_2 is more compatible with the vinyl benzyl alcohol, so we studied this type of nanocomposite (VB–AT series) in detail first. Fig. 4(c) shows the optical properties of the VB–AT series. The refractive index of the VB–AT nanocomposite increases with increasing AA–TiO_2 loading. The experimental data are in good agreement with calculated data. The refractive index is up to 1.73 when the loading of TiO_2 is 18.8 vol%. The results indicate that the short chain length of the acetic acid ligand is not like the long chain length of the hexanoic acid ligand to leave free volume in the nanocomposite. Thus, at a similar TiO_2 loading, using HA–TiO_2 in poly(vinyl benzyl alcohol), the refractive index is reduced to 1.71 for the VB–HT60 sample. On the other hand, using aromatic PAA–TiO_2 to replace AA–TiO_2, the refractive index is increased to 1.77 for the VB–PT60 nanocomposite (Table 2). Indeed, by increasing the aromatic structure of the nanocomposite precursor, we obtain for the first time the highest refractive index transparent thick film reported in the literature according to the best of our knowledge. The optical transparency of VB–AT series nanocomposites is shown in Fig. 5(c). At a low TiO_2 loading of ~5 vol% of the VB–AT20 sample, Rayleigh scattering is observed as seen in E–PT20 and E–HT20. The transmittance is relatively low but is higher than those of E–PT20 and E–HT20. The results confirm the postulation that AA–TiO_2 is relatively compatible with vinyl benzyl alcohol which also can be observed in the TEM image of VB–AT20 (Fig. 6(g)). The transmittance increases with Mie scattering behaviour when the TiO_2 loading is increased to ~10 vol% for the VB–AT40 sample. The aggregation is moderate in VB–AT40 as shown in its TEM image (Fig. 6(h)). When the TiO_2 is increased to 18.8 vol % for the VB–AT60 sample, the transmittance is further increased up to 80% but Rayleigh scattering is observed at wavelengths below 500 nm. The TEM image of VB–AT60 (Fig. 6(i)) shows a small amount of ~10 nm TiO_2 aggregates distributed in the nanocomposite which causes Rayleigh scattering at low wavelengths. Thus, the dispersity of nanoparticles in the polymer matrix is a determining factor for the optical transparency of nanocomposites.

As shown in Table 2, the hardness of the VB–AT series is higher than those of the E–PT and E–HT series because of the increased amount of rigid aromatic structure in the polymer, and the hydrogen bonding formation between the polymer and nanoparticles. The hardness of the VB–AT series increases in the presence of nanoparticles. The increasing extent is larger with higher loading as expected. The results are in good

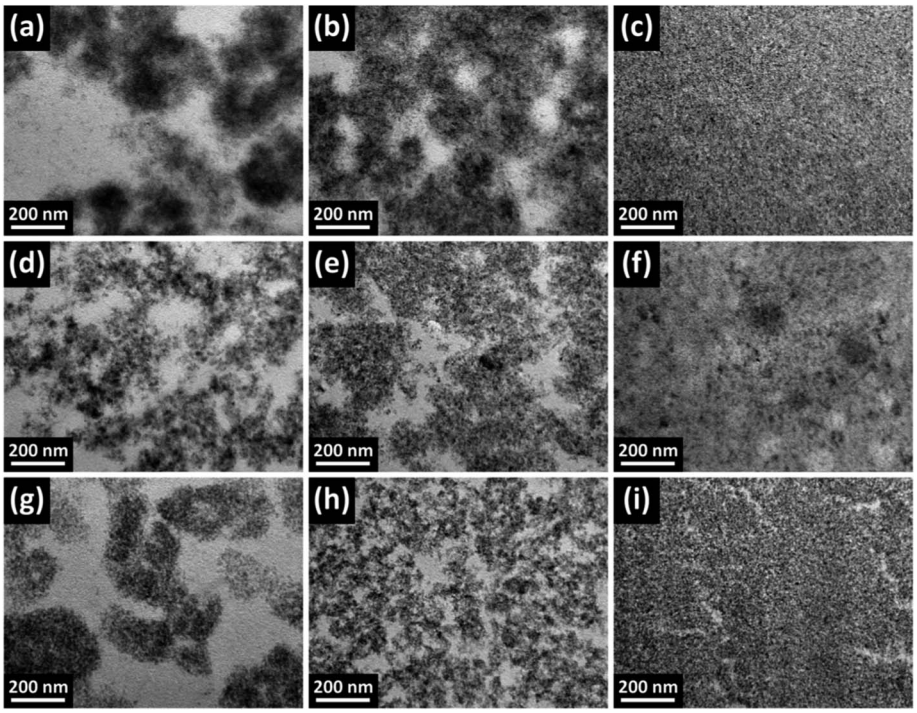

Fig. 6 TEM images of (a) E–HT20, (b) E–HT40, (c) E–HT60, (d) E–PT20, (e) E–PT40, (f) E–PT60, (g) VB–AT20, (h) VB–AT40 and (i) VB–AT60 nanocomposites.

agreement with the literature report of nanocomposites containing nanoparticles chemically bonded with the polymer.[28,29] Thus, the hardness of VB–AT60 is the highest among the samples. The hardness of both VB–PT60 and VB–HT60 is rather low when they are prepared under the same conditions as those of VB–AT60 (75 °C, 24 h). The results may be due to the presence of unreacted monomers. We will discuss the cause of unreacted monomers in the next section.

At low (~5 vol%) AA–TiO_2 loading, the T_d of the VB–AT20 sample is higher than that of neat poly(vinyl benzyl alcohol) which indicates again bond formation between the polymer and nanoparticles (ESI Fig. S4(a)†). However, this phenomenon is not observed in the E–PT20 sample and the E–HT20 sample because there was no chemical bond formation between the polymer and nanoparticles as discussed before. It is surprising to find that the T_d decreases for the AA–TiO_2 loadings higher than ~5 vol% which may be due to the presence of unreacted vinyl alcohol in the sample. The heat of polymerization of nanocomposites is in the decreasing order of VB–PT60 < VB–AT60 < neat vinyl alcohol after the normalization of the polymer content (ESI Fig. S5†). This indicates that unreacted vinyl alcohol is indeed present in the sample which results in lowered T_d and T_g. The lower heat of polymerization of VB–PT60 reveals that the rate of polymerization of VB–PT60 is lower than that of VB–AT60. The result can be rationalized by the larger size of ligand PAA as compared with AA, *i.e.* the reduced effective frequency factor of polymerization. The detailed reaction kinetics of the hybrid system is currently under investigation. The T_g of the VB–AT series increases with increasing the AA–TiO_2 loading as expected from the reduced mobility of the polymer in the presence of nanoparticles upon heating (ESI Fig. S4(b)†). However, both T_d and T_g of VB–AT nanocomposites are lower than those of E–PT and E–HT because the benzylic structure of poly(vinyl benzyl alcohol) makes it less thermally stable than that of polyacrylate.

Conclusions

High refractive index transparent nanocomposites can be achieved by rational design and synthesis of solventless nanocomposite precursors containing a high amount of aromatic structure in the organic matrix and a high content of nanoparticles. At ~18 vol% of anatase TiO_2 nanoparticles, the nanocomposite precursor can be easily processed into a nanocomposite thick film with optimal properties. The polyacrylate nanocomposite made from aromatic PAA-modified TiO_2 has better performance in terms of the refractive index, thermal properties and mechanical properties than that of the nanocomposite containing aliphatic HA-modified TiO_2. The refractive index of the nanocomposite is further increased by using a high aromatic content of poly(vinyl benzyl alcohol) (PBzOH) instead of polyacrylate. At the same 18 vol% of TiO_2, the PVBzOH–AA–TiO_2 nanocomposite has a refractive index of 1.73, a hardness of 30.61 VHN and excellent transparency (>85% from 500 nm to 800 nm). The AA–TiO_2 is acetic acid-modified TiO_2. By replacing aliphatic AA–TiO_2 with PAA–TiO_2, the refractive index of the nanocomposite is increased to 1.77. This solvent free precursor of high refractive index transparent nanocomposites has potential applications in the fabrication of optics and encapsulation of optoelectronic devices.

Acknowledgements

We thank the National Science Council of Taiwan for the financial support for this research (NSC 100-2120-M-002-007 and 101-2120-M-002-003).

References

1 K. C. Krogman, T. Druffel and M. K. Sunkara, *Nanotechnology*, 2005, **16**(7), S338.
2 S. C. Yang, J. S. Kim, J. H. Jin, S. Y. Kwak and B. S. Bae, *J. Appl. Polym. Sci.*, 2011, **122**(4), 2478.
3 F. W. Mont, J. K. Kim, M. F. Schubert, E. F. Schubert and R. W. Siegel, *J. Appl. Phys.*, 2008, **103**(8), 083120.
4 H. W. Su and W. C. Chen, *J. Mater. Chem.*, 2008, **18**(10), 1139.
5 G. S. Liou, P. H. Lin, H. J. Yen, Y. Y. Yu and W. C. Chen, *J. Polym. Sci., Part A: Polym. Chem.*, 2010, **48**(6), 1433.
6 B. Cai, O. Sugihara, H. I. Elim, T. Adschiri and T. Kaino, *Appl. Phys. Express*, 2011, **4**(9), 092601.
7 X. Sun, X. Chen, X. Liu and S. Qu, *Appl. Phys. B: Lasers Opt.*, 2011, **103**(2), 391.
8 M. Russo, M. Campoy-Quiles, P. Lacharmoise, T. A. M. Ferenczi, M. Garriga, W. R. Caseri and N. Stingelin, *J. Polym. Sci., Part B: Polym. Phys.*, 2012, **50**(1), 65.
9 D. Koziej, F. Fischer, N. Kraenzlin, W. R. Caseri and M. Niederberger, *ACS Appl. Mater. Interfaces*, 2009, **1**(5), 1097.
10 J. G. Liu, Y. Nakamura, T. Ogura, Y. Shibasaki, S. Ando and M. Ueda, *Chem. Mater.*, 2008, **20**(1), 273.
11 Y. Imai, A. Terahara, Y. Hakuta, K. Matsui, H. Hayashi and N. Ueno, *Eur. Polym. J.*, 2009, **45**(3), 630.
12 N. Nakayama and T. Hayashi, *Composites, Part A*, 2007, **38**(9), 1996.
13 N. Nakayama and T. Hayashi, *J. Appl. Polym. Sci.*, 2007, **105**(6), 3662.
14 C. C. Chang, L. P. Cheng, F. H. Huang, C. Y. Lin, C. F. Hsieh and W. H. Wang, *J. Sol-Gel Sci. Technol.*, 2010, **55**(2), 199.
15 G. J. Ruiterkamp, M. A. Hempenius, H. Wormeester and G. J. Vancso, *J. Nanopart. Res.*, 2011, **13**(7), 2779.
16 Y. Liu, C. Lue, M. Li, L. Zhang and B. Yang, *Colloids Surf., A*, 2008, **328**(1–3), 67.
17 C. L. Lu, Z. C. Cui, Y. Wang, Z. Li, C. Guan, B. Yang and J. C. Shen, *J. Mater. Chem.*, 2003, **13**(9), 2189.
18 J. L. H. Chau, C. T. Tung, Y. M. Lin and A. K. Li, *Mater. Lett.*, 2008, **62**(19), 3416.
19 J. L. H. Chau, H. W. Liu and W. F. Su, *J. Phys. Chem. Solids*, 2009, **70**(10), 1385.
20 Y. Kurata, O. Sugihara, T. Kaino, K. Komatsu and N. Kambe, *J. Opt. Soc. Am. B*, 2009, **26**(12), 2377.
21 B. T. Liu, S. J. Tang, Y. Y. Yu and S. H. Lin, *Colloids Surf., A*, 2011, **377**(1–3), 138.
22 P. D. Cozzoli, A. Kornowski and H. Weller, *J. Am. Chem. Soc.*, 2003, **125**(47), 14539.
23 Y. Q. Rao, B. Antalek, J. Minter, T. Mourey, T. Blanton, G. Slater, L. Slater and J. Fornalik, *Langmuir*, 2009, **25**(21), 12713.
24 Y. Y. Song, H. Hildebrand and P. Schmuki, *Surf. Sci.*, 2010, **604**(3–4), 346.
25 I. Řehoř, V. Kubíček, J. Kotek, P. Hermann, J. Száková and I. Lukeš, *Eur. J. Inorg. Chem.*, 2011, (12), 1981.
26 C. Kittel, *Introduction to Solid State Physics*, 8th edn, Wiley, 2004.
27 R. He, P. H. Toy and Y. Lam, *Adv. Synth. Catal.*, 2008, **350**(1), 54.
28 C. C. Lin, K. H. Chang, K. C. Lin and W. F. Su, *Compos. Sci. Technol.*, 2009, **69**(7–8), 1180.
29 C. C. Lin, S. H. Hsu, Y. L. Chang and W. F. Su, *J. Mater. Chem.*, 2010, **20**(15), 3084.

